



A Simple Production Method of Mesoporous Titania Nanopowders for Energy Applications

Sorapong Pavasupree^{1,*}, Jaturong Jitputti², Supachai Ngamsinlapasathian²,
Yoshikazu Suzuki², and Susumu Yoshikawa²

¹Department of Materials and Metallurgical Engineering, Faculty of Engineering,
Rajamangala University of Technology Thanyaburi, Klong 6, Pathumthani, 12110, Thailand.

²Institute of Advanced Energy, Kyoto University, Uji, Kyoto 611-0011, Japan.

E-mail: sorapongp@yahoo.com*

Abstract

In this study, mesoporous TiO₂ nanopowders with narrow pore size distribution (pore size about 3-4 nm) and higher surface area (about 180 m²/g) were prepared by hydrothermal method at 130 °C for 12 h. Interestingly, the applications (dye-sensitized solar cell and H₂ production from water-splitting reaction) results of the prepared TiO₂ showed higher efficiency than commercial TiO₂ nanoparticles.

Keywords: Mesoporous, TiO₂, Dye-sensitized Solar Cell, Water splitting.

1. Introduction

In the past decade, mesoporous materials have been of great interest as catalysts because of their unique textural and structural characteristics. Much effort has concentrated on the important metal oxides such as TiO₂, SnO₂, VO₂, and ZnO. Among them, TiO₂ and TiO₂-derived materials are of importance for utilizing solar energy and environmental purification. TiO₂ has been widely used for various applications such as a semiconductor in dye-sensitized solar cell, water treatment materials, catalysts, gas sensors, and so on [1]. Functional properties of TiO₂ are influenced by many factors such as crystallinity, particle size, surface area, and preparation. Hydrothermal synthesis has become one of the most important and promising new material fabrication method for nanoscale materials and nanotechnology [2-7]. In our previous works, mesoporous TiO₂ were synthesized by a modified sol-gel method, however, the prepared mesoporous TiO₂ had surface area about 80 m²/g [8-10].

In this study, mesoporous anatase TiO₂ nanopowders with narrow pore size distribution (pore size about 3-4 nm) and higher surface area (about 193 m²/g) has been synthesized, which shows high photocatalytic activity and high performance in dye-sensitized solar cell. The detail microstructure, photocatalytic, and photovoltaic properties will be reported.

2. Experimental Procedure

2.1 Synthesis

Titanium (IV) butoxide (Aldrich) was mixed with the same mole of acetylacetone (ACA, Nacalai Tesque, Inc., Japan) to slowdown the hydrolysis and the condensation reactions [11-13]. Subsequently, distilled water 40 ml was added in the solution, and the solution was stirred at room temperature for 5 min. After kept stirring, the solution was put into a Teflon-lined stainless steel autoclave and heated at 130 °C for 12 h with stirring condition. After the autoclave was naturally cooled to room temperature, the obtained product was washed with 2-propanol and distilled water, followed by drying at 100 °C for 12 h.

2.2 Characterization

The crystalline structure of the samples was evaluated by X-ray diffraction (XRD, RIGAKU RINT 2100). The microstructure of the prepared materials was analyzed by scanning electron microscopy (SEM, JEOL JSM-6500FE), transmission electron microscopy (TEM, JEOL JEM-200CX), and selected-area electron diffraction (SAED). The Brunauer-Emmett-Teller (BET) specific surface area was determined by the nitrogen adsorption (BEL Japan, BELSORP-18 Plus).

2.3 Dye-sensitized solar cell measurement

TiO₂ electrodes were prepared as follows; 1 g of TiO₂ powder was mixed with 0.1 mL of ACA, and was ground mechanically. During vigorous stirring, 5 ml of mixture of water and ethanol (1:1, in vol %) was added and 0.4 ml of polyoxethylene (10) octylphenyl ether (Triton x-100) was added to facilitate spreading of the paste on the substrate. The obtained colloidal paste was coated on fluorine-doped SnO₂ conducting glass (FTO, sheet resistance 15 Ω/□, Asahi glass Co., Ltd.) by squeegee technique. After coating, each layer was dried at room temperature and then annealed at 400 °C for 5 min. The coating process was repeated to obtain thick films. The resulting films were sintered at 450 °C for 2 h in air.

Sintered TiO₂ electrodes were soaked in 0.3 mM of ruthenium (II) dye (known as N719, Solaronix) in a *t*-butanol/ acetonitrile (1:1, in vol %) solution. The electrodes were washed with acetonitrile, dried, and immediately used for measuring photovoltaic properties. The electrolyte was composed of 0.6 M dimethylpropylimidazolium iodide, 0.1 M lithium iodide (LiI), 0.05 M iodide (I₂), and 0.5 M 4-*tert*-butylpyridine in acetonitrile.

The thickness of the TiO₂ films was measured with a Tencor Alpha-step Profiler. Photocurrent-voltage curve was measured under simulated solar light (CEP-2000, Bunkoh-Keiki, AM 1.5, 100 mW/cm²). The light intensity of the illumination source was calibrated by using a standard silicon photodiode (BS520, Bunkoh-Keiki).

The amount of adsorbed dye was determined by desorbing the dye from the titania surface into a mixed solution of 0.1 M NaOH and ethanol (1:1 in volume fraction) and measuring its absorption spectrum. The concentration of adsorbed dye was analyzed by UV-vis spectrophotometer (UV-2450 SHIMADZU).

2.4 Photocatalytic hydrogen production

Photocatalytic H₂ production reaction was carried out in a closed gas-circulation system (Fig. 1). TiO₂ photocatalyst (0.8 g) was suspended in aqueous methanol solution (800mL distilled H₂O, 80mL methanol) by means of magnetic stirrer within an inner irradiation-type reactor (1100 mL) made of Pyrex glass. A high-pressure Hg lamp (Ushio; UM-452, 450 W) was utilized as the light source. Prior to the reaction, the mixture was deaerated by purging with Ar gas repeatedly. To maintain the reaction temperature during the course of reaction, cooling water was circulated through a cylindrical Pyrex jacket located around the light source. The gaseous H₂ produced was periodically analyzed by an on-line gas chromatograph (Shimadzu GC-8A, Molecular sieve 5A, TCD, Ar carrier).

3. Results and Discussion

3.1 Characterization results [17]

Figure 1 shows the X-ray diffraction pattern of the as-synthesized sample. The peaks were rather sharp, which indicated the obtained TiO₂ had relatively high crystallinity, and attributable to the anatase phase.

Figure 2 gives the nitrogen adsorption isotherm and the pore size distribution of the as-synthesized sample. The isotherm shows a typical IUPAC type IV pattern with inflection of nitrogen adsorbed volume at P/P₀ about 0.50 (type H₂ hysteresis loop), indicating the existence of mesopores. The pore size distribution of the sample, as shown in the inset of Figure 2, showed that the as-synthesized sample had average pore diameter about 4-5 nm. The BET surface area and pore volume of sample are about 193 m²/g and

0.286 cm³/g, respectively (higher than the previous works (ref. 8-10, 80 m²/g) about 2 times).

SEM and TEM images of the as-synthesized sample showed nanoparticles size about 5 nm (Figure 3-4). The electron diffraction pattern shown in the inset of (Figure 4) supported that the as-synthesized sample was anatase-type TiO₂. The lattice fringes of the nanorods and the nanoparticles appearing in the image (*d* = 0.35 nm) also allowed for the identification of the anatase phase (Figure 5). HRTEM images of the as-synthesized sample with clear lattice fringes, again confirming its high crystallinity.

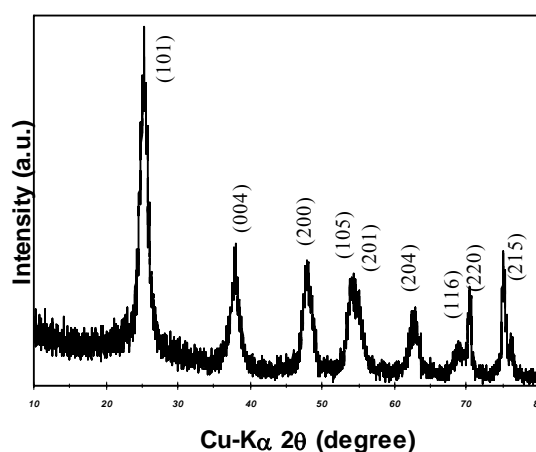


Figure 1. X-ray diffraction pattern of the as-synthesized mesoporous anatase TiO₂ nanopowders.

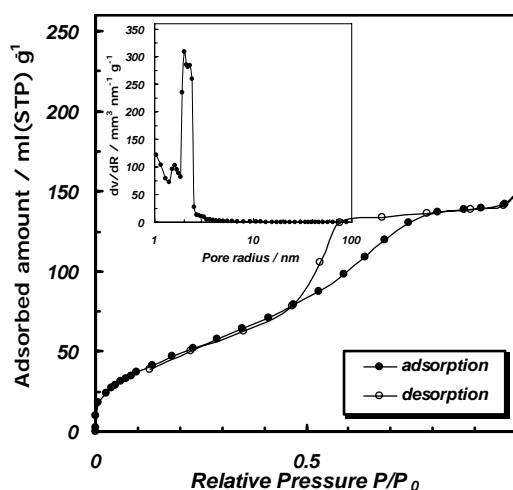


Figure 2. Nitrogen adsorption isotherm pattern of the as-synthesized mesoporous anatase TiO₂ nanopowders, and the pore size distribution of the sample with pore diameter about 4-5 nm (inset).

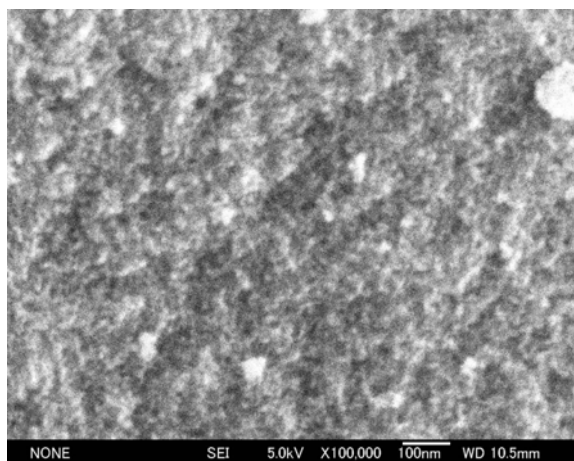


Figure 3. SEM image of the as-synthesized mesoporous anatase TiO₂ nanopowders.

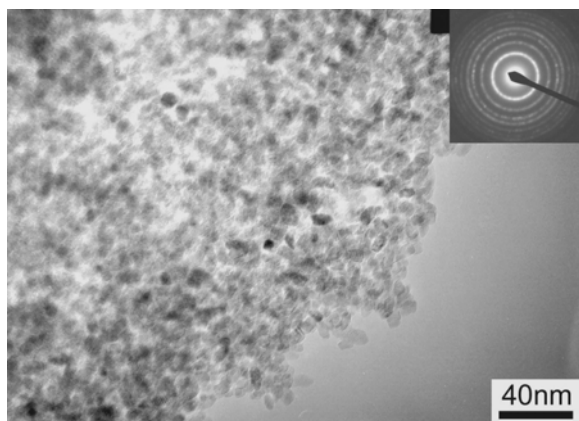


Figure 4. TEM and SAED images of the as-synthesized mesoporous anatase TiO₂ nanopowders.

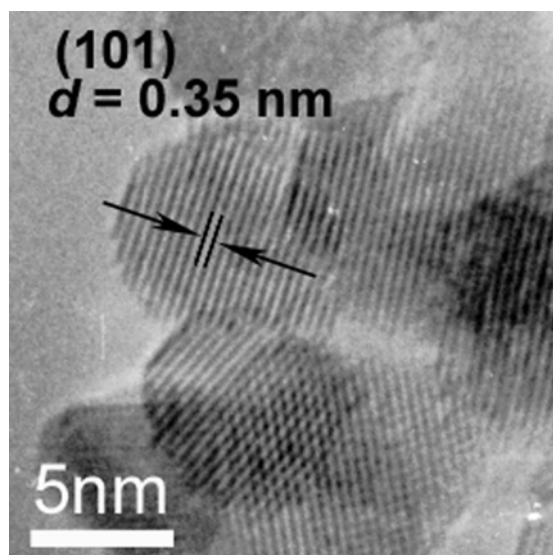


Figure 5. HRTEM of the as-synthesized mesoporous anatase TiO₂ nanopowders.

3.2 Dye-sensitized solar cell results [17]

Table 1 shows the comparison between photocurrent–voltage characteristics of the cell using the mesoporous anatase TiO₂ nanopowders (thickness = 10.0 μm) and P-25 (thickness = 13.8 μm). The solar energy conversion efficiency of the cell using the mesoporous anatase TiO₂ nanopowders was about 6.30 % with J_{sc} of 13.28 mA/cm², V_{oc} of 0.702 V and ff of 0.676; while η of the cell using P-25 reached 5.82 % with J_{sc} of 12.74 mA/cm², V_{oc} of 0.704 V and ff of 0.649. Higher current density and efficiency might be attributed to higher amount of adsorbed dye (10.21 × 10⁻⁸ mol/cm² for the mesoporous anatase TiO₂ nanopowders and 5.68 × 10⁻⁸ mol/cm² for P-25), owing to larger surface area of the mesoporous anatase TiO₂ nanopowders (Table 2).

Table 1 The photocurrent-voltage characteristic of a typical dye sensitized solar cells fabricated by the mesoporous anatase TiO₂ nanopowders and commercial TiO₂ nanoparticles (P-25).

Samples	J _{sc} (mA/cm ²)	V _{oc} (V)	η (%)
Prepared TiO ₂	13.28	0.702	6.30
P-25	12.74	0.704	5.82

Table 2 The BET surface area and amount of adsorbed dye of the mesoporous anatase TiO₂ nanopowders (prepared by this study) calcined at 450 °C for 2 h and P-25 calcined at 450 °C for 2 h.

Samples	BET surface area (m ² /g)	Amount of adsorbed dye (mol/cm ²)
Prepared TiO ₂	101	10.21 × 10 ⁻⁸
P-25	54	5.68 × 10 ⁻⁸

Figure 6 (a, c) depict the nitrogen adsorption-desorption isotherms and pore size distributions of the mesoporous anatase TiO₂ nanopowders calcined at 450 °C for 2 h. The isotherms exhibit typical type IV pattern with hysteresis loop, characteristic of mesoporous material according to the classification of IUPAC. A sharp increase in adsorption volume of N₂ was observed and located in the P/P₀ range of 0.70-0.85. This sharp increase can be imputable to the capillary condensation, indicating the good homogeneity of the sample and fairly small pore size since the P/P₀ position of the inflection point is related to the pore dimension. The pore size distribution obtained by BJH approach (Figure 6 (c)) is noticeably narrow, confirming good quality of the sample. In comparison, the isotherm of the P-25 after calcined at 450 °C for 2 h is also shown in Figure 6 (b). It can be seen that the isotherm elucidates the typical IUPAC type II pattern, revealing the absence of mesoporous structure in the commercial nanoparticles P-25. The BET surface area of the mesoporous anatase TiO₂ nanopowders and P-25 were around 101 and 54 m²/g, respectively. Second, electron transport of anatase

structure faster than rutile structure [16]. The crystalline structure of the mesoporous anatase TiO₂ nanopowders calcined at 450 °C for 2 h was anatase, while P-25 calcined at 450 °C for 2 h was a mixture of anatase and rutile (Figure 7).

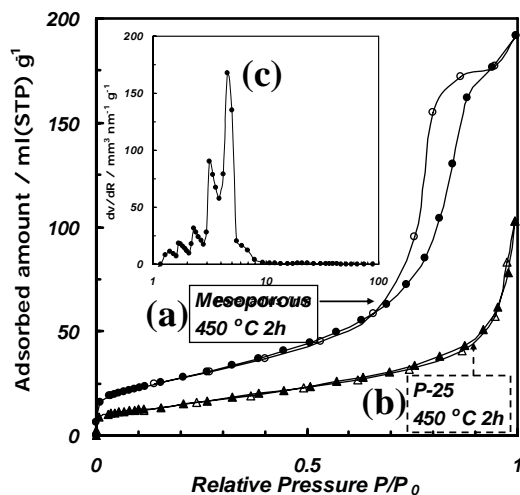


Figure 6 (a) Nitrogen adsorption isotherm pattern of the mesoporous anatase TiO₂ nanopowders calcined at 450 °C for 2 h, BET surface are 134 m²/g, (b) P-25 (450 °C for 2 h, BET surface are 54 m²/g), and (c) the pore size distribution of the mesoporous anatase TiO₂ nanopowders with pore diameter about 6-10 nm.

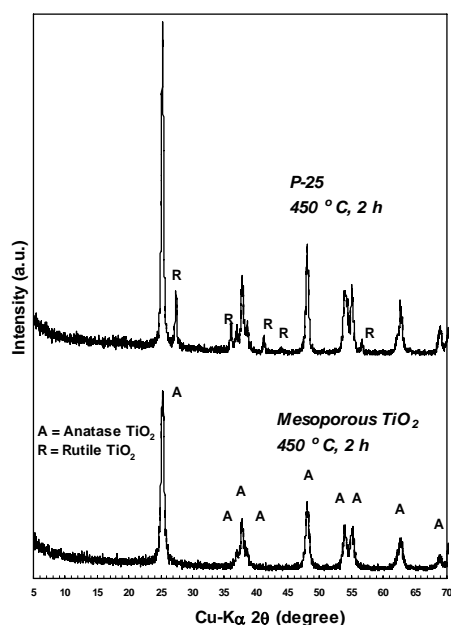


Figure 7. X-ray diffraction patterns of the mesoporous anatase TiO₂ nanopowders calcined at 450 °C for 2 h and P-25 calcined at 450 °C for 2 h.

3.3 H₂ production from water splitting reaction results [18]

Figure 8 demonstrates the time course of the photocatalytic H₂ production from water splitting reaction over the mesoporous TiO₂ calcined at various temperature and commercial TiO₂ nanoparticles (ST-

01). The photocatalytic H₂ evolution activity of the calcined mesoporous TiO₂ samples were higher than the commercial TiO₂ nanoparticles (ST-01). In our previous works, it is obviously revealed that the introduction of mesopore into titania photocatalyst substantially improved the photocatalytic performance [15, 18].

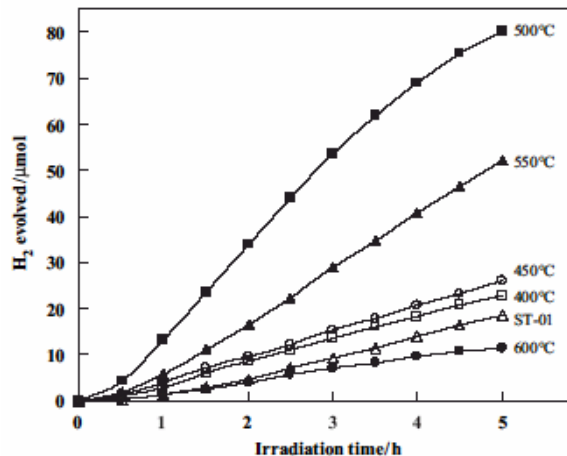


Figure 8. Photocatalytic H₂ production from water-splitting reaction over the mesoporous TiO₂ calcined at various temperatures and commercial TiO₂ (Ishihara ST-01).

5. Conclusion

In summary, high surface area (about 180 m²/g) anatase TiO₂ with mesoporous structure (pore diameter about 3-4 nm) was synthesized by hydrothermal method at 130 °C for 12 h. The η of the cell using mesoporous anatase TiO₂ nanopowders (prepared by this study) was about 6.30 %, while η of the cell using P-25 reached 5.82 %. Mesoporous anatase TiO₂ nanopowders showed higher photocatalytic activity than the commercial TiO₂ (ST-01). This synthesis method provided a simple route to fabricate mesoporous anatase TiO₂ nanopowders with mild condition. The results clearly showed that the mesoporous TiO₂ (prepared by this method) is the promising candidate to serve as an energy-related material.

Acknowledgments

The authors would like to express gratitude to Prof. S. Isoda and Prof. H. Kurata, Institute for Chemical Research, Kyoto University for the use of TEM apparatus Prof. T. Yoko, Institute for Chemical Research, Kyoto University for the use of XRD equipment. Prof. Mochizuki at AIST for the kind supply of Pt counter electrode. We are also grateful to the Geomatec Co. Ltd. for providing a part of conducting glass. This work was supported by grant-in-aids from the Ministry of Education, Science Sports, and Culture of Japan under the 21 COE program, the Nanotechnology Support Project, NEDO under high-performance dye-sensitized solar cell project, and from JSPS research fellow.

References

- [1] Fujishima, A., Rao, T. N. and Tryk, D. A. (2000) Titanium dioxide photocatalysis, *J. Photochem. Photobiol. C:Photochem. Rev.*, **1**, pp. 1-21.
- [2] Pavasupree, S., Suzuki, Y., Kitiyanan, A., Pivsa-Art, S. and Yoshikawa, S. (2005) Synthesis and characterization of vanadium oxides nanorods, *J. Solid State Chem.*, **178**, pp. 2152-2158.
- [3] Suzuki, Y., Pavasupree, S., Yoshikawa, S. and Kawahata, R. (2005) Natural rutile-derived titanate nanofibers prepared by direct hydrothermal processing, *J. Mater. Res.*, **20**, pp. 1063-1070.
- [4] Pavasupree, S., Suzuki, Y., Yoshikawa, S. and Kawahata, R. (2005) Synthesis of titanate, TiO₂ (B), and anatase TiO₂ nanofibers from natural rutile sand, *J. Solid State Chem.*, **178**, pp. 3110-3116.
- [5] Pavasupree, S., Suzuki, Y., Pivsa-Art, S. and Yoshikawa, S. (2005) Synthesis and characterization of nanoporous, nanorods, nanowires metal oxides, *Sci. Tech. Adv. Mater.*, **6**, pp. 224-229.
- [6] Pavasupree, S., Ngamsinlapasathian, S., Nakajima, M., Suzuki, Y. and Yoshikawa, S. (2006) Synthesis, characterization, photocatalytic activity and dye-sensitized solar cell performance of nanorods/nanoparticles TiO₂ with mesoporous structure, *J. Photochem. Photobiol. A: Chem.*, **184**, pp. 163-169.
- [7] Pavasupree, S., Ngamsinlapasathian, S., Suzuki, Y. and Yoshikawa, S. (2006) Synthesis and dye-sensitized solar cell performance of nanorods/nanoparticles TiO₂ from high surface area nanosheet TiO₂, *J. Nanosci. Nanotech.*, **6**, pp. 3685-3692.
- [8] Pavasupree, S., Suzuki, Y., Pivsa-Art, S. and Yoshikawa, S. (2005) Preparation and characterization of mesoporous MO₂ (M=Ti, Ce, Zr, and Hf) nanopowders by a modified sol-gel method, *Ceram. Int.*, **31**, pp. 959-963.
- [9] Pavasupree, S., Suzuki, Y., Pivsa-Art, S. and Yoshikawa, S. (2005) Preparation and characterization of mesoporous TiO₂-CeO₂ nanopowders respond to visible wavelength, *J. Solid State Chem.*, **178**, pp. 128-134.
- [10] Kitiyanan, A., Ngamsinlapasathian, S., Pavasupree, S. and Yoshikawa, S. (2005) The preparation and characterization of nanostructured TiO₂-ZrO₂ mixed oxide electrode for efficient dye-sensitized solar cells, *J. Solid State Chem.*, **178**, pp. 1044-1048.
- [11] Adachi, M., Murata, Y., Harada, M. and Yoshikawa, S. (2000) Formation of titania nanotubes with high photo-catalytic activity, *Chem. Lett.*, **8**, pp. 942-943.
- [12] Adachi, M., Okada, I., Ngamsinlapasathian, S., Murata, Y. and Yoshikawa, S. (2002) Dye-sensitized solar cell using semiconductor thin film composed of titania nanotubes, *Electrochemistry*, **70**, pp. 449-452.
- [13] Adachi, M., Murata, Y., Okada, I. and Yoshikawa, S. (2003) Formation of titania nanotubes and applications for dye-sensitized solar cells, *J. Electrochem. Soc.*, **150**, (8), pp. G488-G493.
- [14] Sakulkhaemaruechai, S., Pavasupree, S., Suzuki, Y., and Yoshikawa, S. (2005) Photocatalytic activity of titania nanocrystals prepared by surfactant-assisted templating method—effect of calcination conditions, *Mater. Lett.*, **59**, pp. 2965-2968.
- [15] Sreethawong, T., Suzuki, Y. and Yoshikawa, S. (2005) Synthesis, characterization, and photocatalytic activity for hydrogen evolution of nanocrystalline mesoporous titania prepared by surfactant-assisted templating sol-gel process, *J. Solid State Chem.*, **178**, pp. 329-338.
- [16] Park, N.-G., van de Lagemaat, J. and Frank, A.J. (2000) Comparison of dye-sensitized rutile- and anatase-based TiO₂ solar cells, *J. Phys. Chem. B*, **104**, pp. 8989-8994.
- [17] Pavasupree, S., Jitputti, J., Ngamsinlapasathian, S., Suzuki, Y. and Yoshikawa, S. (2007) Hydrothermal synthesis, characterization, photocatalytic activity and dye-sensitized solar cell performance of mesoporous anatase TiO₂ nanopowders, *Materials Research Bulletin*, in press.
- [18] Jitputti, J., Pavasupree, S., Suzuki, Y. and Yoshikawa, S. (2007) Synthesis and photocatalytic activity for water-splitting reaction of nanocrystalline mesoporous titania prepared by hydrothermal method, *J. Solid State Chem.*, **180**, pp. 1743-1749.